ANALYZING AND EXPLORING A MODEL FOR HIGH-EFFICIENCY PEROVSKITE SOLAR CELLS

Mohammed M. Shabat[1,2], Mahassen H. Elblbeisi[1], Guillaume Zoppi[2]

[1] Department of Physics, The Islamic University of Gaza, P.O. Box 108, Gaza Strip, Palestine

[2]Department of Mathematics, Physics & Electrical Engineering, Northumbria University, Newcastle upon Tyne, NE1 8ST, United Kingdom

Abstract. Perovskite materials have drawn a lot of interest recently due to their potential to increase solar cell efficiency. This study uses the solar cell capacitance simulator (SCAPS-1D) to develop and simulate a perovskite solar cell made of semiconductor materials. The design that has been suggested is Al: ZnO/ ZnO/ CdS/ $CsSnCl_3$/ and MoS_2. The analysis focuses on how different characteristics of the material affect the device's performance. The analysis of the data reveals that the architecture had 26.15% power conversion efficiency (PCE). The solar cell provides interest develop a non-toxic solar cell, with low manufacturing costs, outstanding conversion efficiency, and stability.

Keywords Perovskite, Solar cell, high efficiency, $CSSnCl_3$, electrical properties, SCAPS.

1. INTRODUCTION

In the field of photovoltaics, the investigation of $CSSnCl_3$ perovskite-type for solar cell applications has become an interesting area of study [1,2]. A lot of interest has been spent on perovskite solar cells (PSCs) because of their high power conversion efficiency (PCE) and inexpensive manufacturing methods [3-5]. PSC performance and stability can be further enhanced by using materials of the $CSSnCl_3$ perovskite-type, which is an exciting prospect [6, 7]. Materials of the $CSSnCl_3$ perovskite type offer special qualities that make them appropriate for use in solar cells. Because of the tunable bandgaps made possible by their crystal structure, they can effectively absorb light over a large portion of the solar spectrum. This wide absorption spectrum increases the solar cell's total energy conversion efficiency and maximizes the use of incident sunlight [3, 8]. The high charge carrier mobility and diffusion lengths of $CSSnCl_3$ perovskite-type materials, in addition to their tunable bandgap, are essential for effective charge transport inside the solar cell device. These characteristics help to minimize recombination losses and enhance device performance by enabling the effective collection and extraction of photogenerated charges [1, 9]. The low cost and solution-processability of $CSSnCl_3$ perovskite-type materials are additional advantages. In comparison to conventional silicon-based devices, large-scale manufacture of solar cells is possible thanks to easy and scalable fabrication techniques like spin-coating and inkjet printing. The $CSSnCl_3$ perovskite-type materials have the potential for commercialization and wide-scale use of solar energy technologies because of their affordability [2, 9].

These previous studies indicate that additional research is required to fully understand the potential of $CsSnI_3$ as an active component in solar cells [1-9]. So, a thorough examination of $CSSnCl_3$ perovskite-type solar cells' electrical characteristics is required to fully understand their potential. This examination includes investigating their series and shunt resistance as well as the absorber, and buffer layers. Examining these qualities offers important insights into the elements influencing the functionality, effectiveness, and long-term stability of the technology. We aim to broaden our understanding of the characteristics of $CSSnCl_3$ perovskite-type materials and to exploit their full potential for efficient and economical solar energy conversion. With the use of the knowledge obtained through this study, high-performance perovskite solar cells may be designed and made, aiding in the creation of renewable and sustainable energy sources.

2. SIMULATION METHODOLOGY

The numerical simulation program, 1D-SCAPS (version 3.3.05), has been utilized extensively for the theoretical study of 1D solar cells which was developed by the Electronics and Information Systems Department at the University of Gent in Belgium (ELIS) [8]. This simulation tool enables examination of the transport properties of various crystalline, amorphous, or polycrystalline solar cell materials, including bulk flaws and interfaces, by solving the Poisson equation for both electrons and holes at the interface and between the different layers of the device structure. To numerically model the thin-film solar cell, optical and electrical properties of each layer were obtained from literature sources, with simulation parameters set to a working temperature of 300 K and 10^6 ohms in series resistance and 1 ohm in shunt resistance, respectively. Figure (1) depicts the simulated solar cell device, which is made up of layers of Al: ZnO, ZnO, CdS, $CsSnCl_3$, and MoS_2, with Al: ZnO serving as the window layers, $CsSnCl_3$ perovskite serving as the absorber layer, CdS serving as the buffer layer, and MoS_2 serving as the back contact. The work function was considered as a flat band in the entire simulation, with SCAPS automatically computing the work function to establish an ohmic contact [10]. It should be emphasized that this simulated study did not take the effect of dangling bonds on material contacts.

Figure1. The suggested perovskite solar cell.

Table 1

Solar cell absorption materials parameters used in the simulation [1, 11-14].

Parameters (Absorber layers)	**$CsSnCl_3$**
Thickness (nm)	800
Band gap, E_g (eV)	1.52
Electron affinity, *X* (eV)	3.90
Dielectric permittivity (relative), ε_r	29.4
CB effective density of states, NC ($1/cm^3$)	1×10^{19}
VB effective density of states, NV ($1/cm^3$)	1×10^{19}
Electron mobility, μn (cm^2 /Vs)	2
Hole mobility, μh (cm^2 /Vs)	2
Shallow uniform acceptor density, NA ($1/cm^3$)	1×10^{15}
Shallow uniform donor density, ND ($1/cm^3$)	0
Defect density, Nt ($1/cm^3$)	1×10^{15}

Table2

Window layer, buffer layer, and back contact materials parameters are used in the simulation [10].

Parameter	MoS_2	CdS	ZnO	Al:ZnO
Thickness	100	80	80	200
Band gap	1.7	2.4	3.3	3.37
Electron affinity	4.2	4.2	4.6	4.6
Dielectric permittivity	13.6	9	9	9
CB effective density of states (cm^{-3})	2.2E+18	2.2E+19	2.2E+19	1 E+21
VB effective density of states (cm^{-3})	1.8E+19	1.8E+18	1.8E+19	1 E+20
Electron thermal velocity (cms^{-1})	1.0E+7	1.0E+7	1.0E+7	1.0E+7
Hole thermal velocity (cms^{-1})	1.0E+7	1.0E+7	1.0E+7	1.0E+7
Electron mobility (cm^2/V_s)	100	100	100	150
Hole mobility (cm^2/V_s)	25	25	25	25
Shallow uniform donor density, N_D (cm^{-3})	0	3.0E+16	1.0E+14	1E+20
Shallow uniform acceptor density, N_A (cm^{-3})	1.0E+16	1.0E+1	1.0E+1	0

4. RESULTS AND DISCUSSIONS

We conducted an analytical study of the $CsSnCl_3$ perovskite solar cell. The primary focus of the study was to investigate the electrical property of the cell and their relationship with series and shunt resistance, the absorber layer, the buffer layer, acceptor density, and the temperature. The device structure used in the study was a hetero-structure of Al: ZnO/ ZnO/ CdS/ perovskite/ and MoS_2.

Two important factors, series resistance (Rs) and shunt resistance (Rsh), affect a solar cell's electrical characteristics. In this part, we examine how series and shunt resistances affect electrical properties. The effects of series resistance are examined in power conversion efficiency (PCE), short circuit currant (Jsc), open circuit voltage (Voc), and fill factor (FF) in Figure 2. Here, the series resistance changes from (0–6) Ohm.

As series resistance rises, the fill factor and power conversion efficiency decline. The resistance in the conducting medium of the solar cell is referred to as the series resistance, which includes the resistance of the materials and connections. As current passes through it, it causes a voltage to drop, which lowers power production and efficiency.

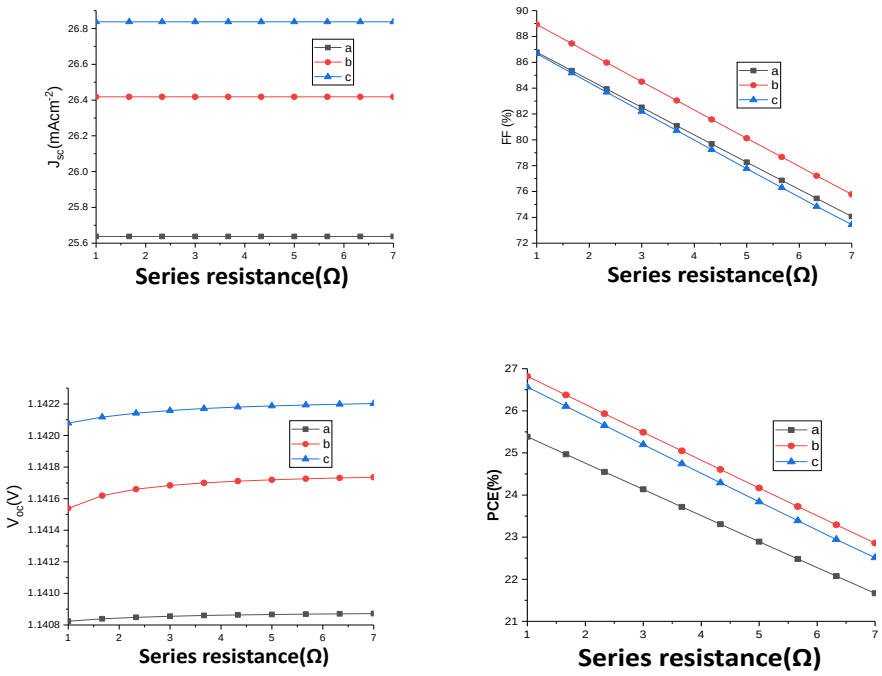

Figure2. Effect of series resistance on various electrical characteristics (a=0.6 µm, c= 1µm, b= 0.8).

The short current density remains constant even though the series resistance rises but the open voltage rises up to 1.1422 volts.

Figure 3 shows how RSh effects in the range of 0-10^7 Ohm. The figure shows the significantly different PV parameter values for VOC, JSC, FF, and PCE for various shunt resistances. When RSh rises from 0 to $2x10^6$ Ωcm^2, all characteristics increase dramatically.

The PCE reached the highest value of 27% at RSh of $2x10^6$ and remained constant up to 10^7 Ω cm^2 or beyond RSh. The primary origin of RSh is the defects formed during the manufacturing process. The structure becomes a low-resistance path for current flow at a higher RSh value. Herein, the V_{OC} increased with shunt resistance up to 1.1 volts while the J_{SC} was found up to 27 mA/cm^2.

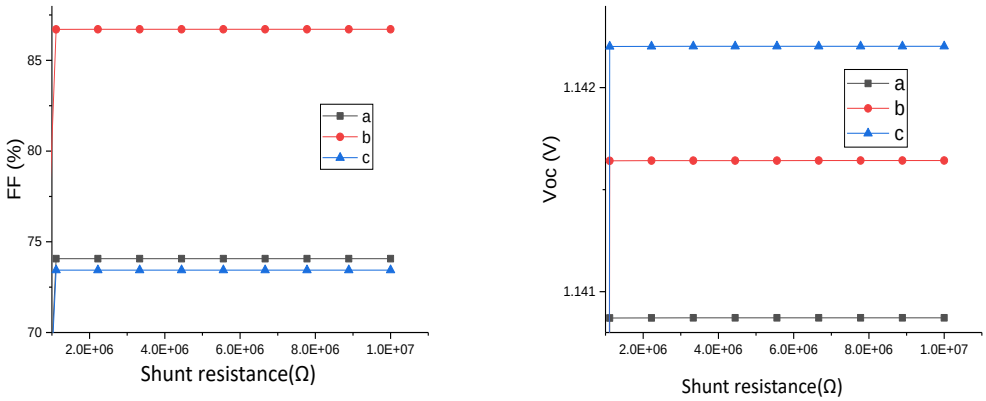

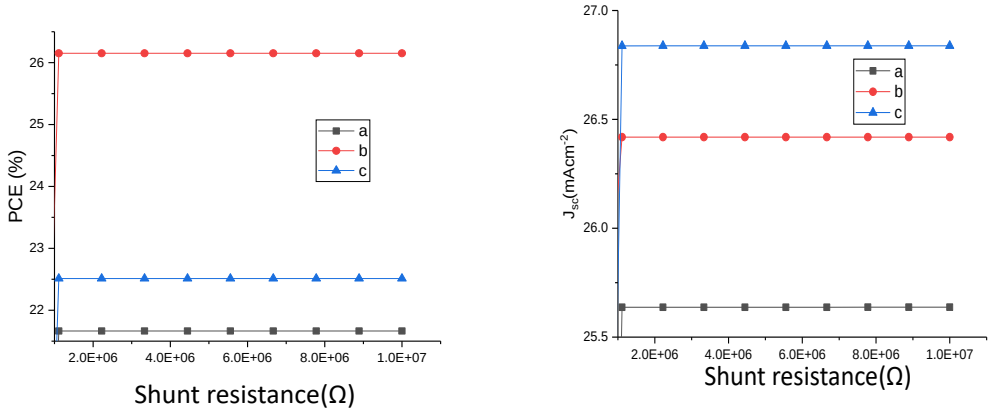

Figure 3. Effect of Shunt resistance on various electrical characteristics (**a=0.6 µm, c= 1µm, b= 0.8)**

These results agree with other papers that study the resistance effect on other suggested cells with different layers but with better results for this cell [1].

4.1 Buffer layer analysis

When used as a buffer layer in solar cells, cadmium sulfide (CdS) has a variety of effects on the electrical characteristics. First, due to the energy band structure's capacity for proper energy level alignment, charge carrier extraction and injection at interfaces are made possible. Additionally, CdS aids in the creation of electron-hole pairs by absorbing visible light. A steady current flow is ensured by the high electron mobility of CdS, which enables efficient electron transport from the light-absorbing layer to the electrode. In addition, CdS functions as a surface passivation layer, lowering charge carrier recombination at interfaces and enhancing carrier lifespan. Additionally, CdS serves as a buffer between the transparent conducting oxide electrode and the light-absorbing layer, maximizing energy level alignment, enhancing carrier extraction, and decreasing interfacial barriers [15, 16]. The actual effect of CdS on electrical characteristics depends on several variables, including its thickness, the process used for deposition, and the components and structure of the solar cell.

Here, the effect of the buffer layer's thickness on a solar cell parameter with various absorber layer thicknesses has been investigated. Figure 2 illustrates the impact of changing the buffer layer's thickness on the performance of the solar cell.

Figure. 4 shows that the J_{sc}, and V_{oc} are essentially constant concerning the thickness of the buffer layer but PCE, and FF decrease. To reduce the series resistance, buffer layers should generally be as thin as possible. Low charge separation between the photogene-rated carriers is caused by the very thin buffer layer's tiny space charge width [10]. A very thin buffer layer also causes a greater leakage current. This is seen in PCE results with a buffer layer ranging in thickness from 0.02 to 0.08 nm.

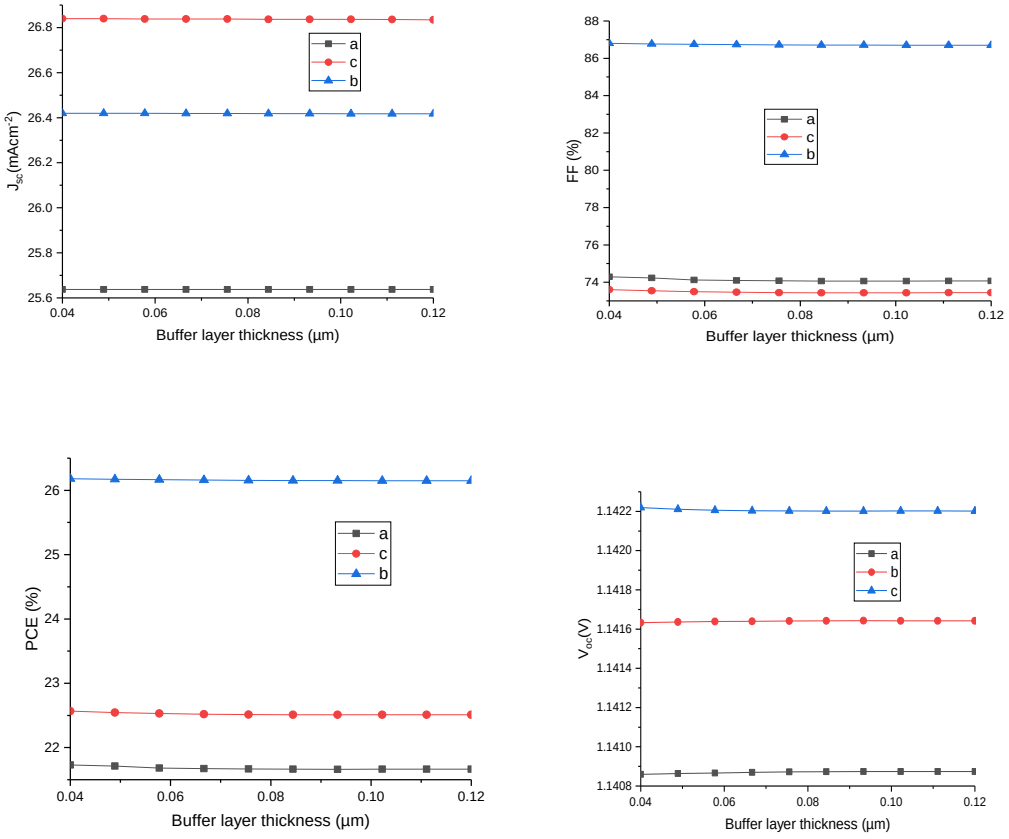

Figure 4. The variation of buffer layer thickness and corresponding change in electrical parameters of solar cell.(a=0.6 µm, c= 1µm, b= 0.8)

The effect of the buffer layer doping concentration on solar cell characteristics with three different absorber layer thicknesses is examined in this section. The solar cell's output performance changes in Figure. 5 when the buffer layer's doping concentration (measured in cm^{-3}) increases. From figure

5, it can be seen that the electrical parameters FF and V_{oc} with different solar cell device structures change relatively little as the electron concentration varies (3x 10^{18} to 9 x10^{18}). As concentration rises, PCE, and J_{sc} decline.

Increasing the doping concentration of CdS as a buffer layer in a solar cell can lead to a decrease in the power conversion efficiency (PCE) and short-circuit current (J_{sc}). This can be attributed to several factors. Firstly, higher doping concentrations introduce additional defects and recombination centers, increasing the rate of charge carrier recombination and reducing the overall efficiency of the device. Secondly, increased doping can elevate the series resistance within the solar cell, impeding the flow of current and resulting in a lower J_{sc} [17]. Additionally, excessive doping can alter the optical properties of the CdS layer, limiting the absorption of photons and reducing the generation of electron-hole pairs, leading to a decrease in J_{sc}. Lastly, higher doping concentrations may also reduce the carrier mobility within the CdS layer, hindering the efficient transport of charge carriers and resulting in a lower J_{sc} [18-20]. Therefore, optimizing the doping concentration is crucial to maintaining high PCE and J_{sc} in CdS-based solar cells.

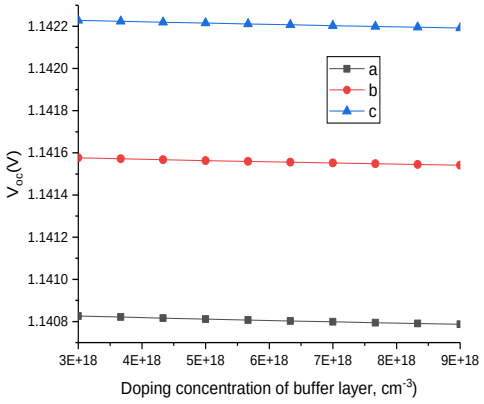

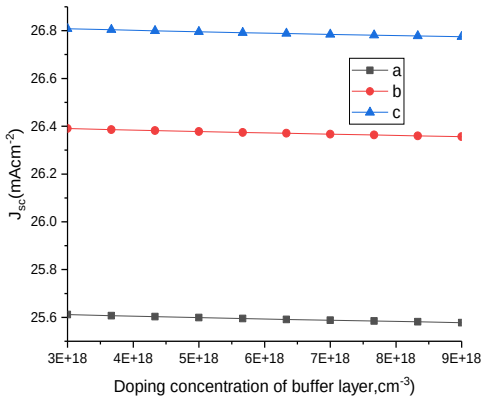

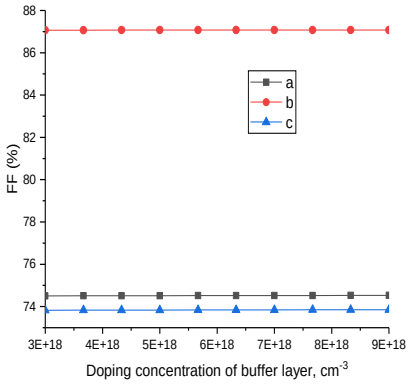

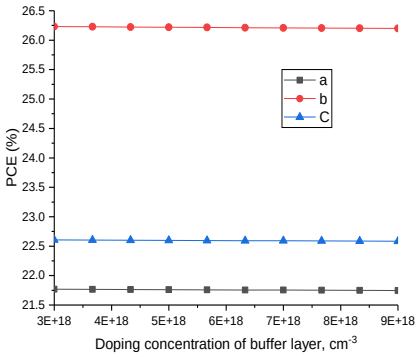

Figure 5. The impact of buffer layer doping concentration (a=0.6 µm, c= 1µm, b= 0.8).

4.2 $CSSnCl_3$ absorber layer analysis

Figure 6 illustrates the impact of temperature on various electrical parameters, where it can be observed that an increase in temperature causes a decrease in both V_{oc} and FF, while PCE and J_{sc} remain unaffected. The open-circuit voltage is the parameter most affected by the temperature increase, following previous studies that highlight the dependence of photovoltaic solar cells on temperature sensitivity and open-circuit voltage [10]. Higher-voltage solar cells exhibit less temperature sensitivity, which emphasizes the importance of considering the open-circuit voltage when assessing a solar cell's temperature performance.

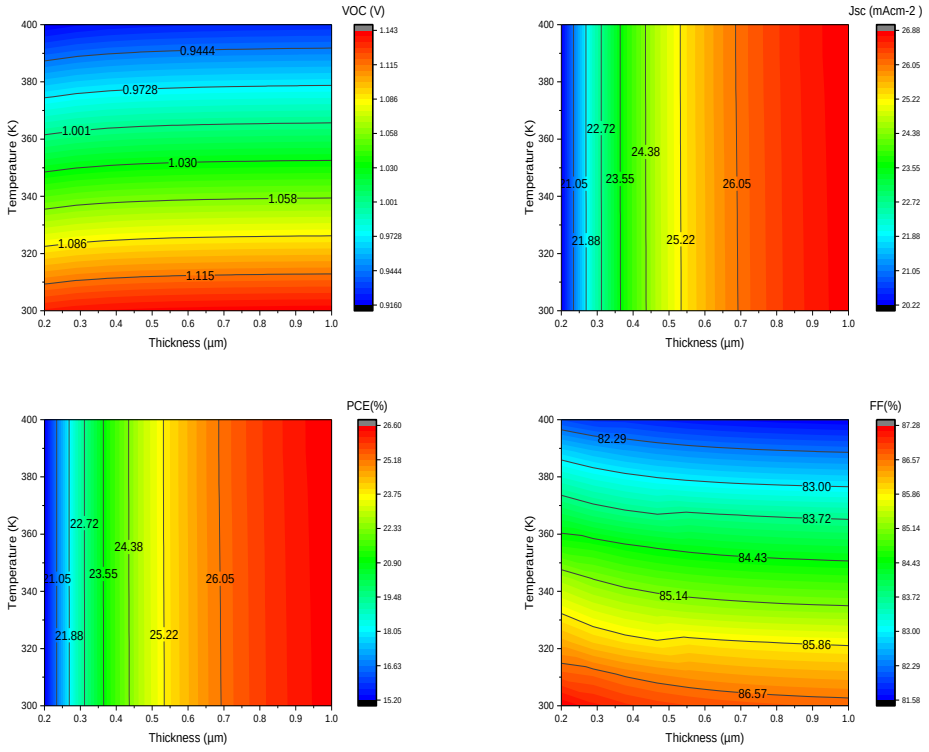

Figure 6. Contour graph the variation of $CSSnCl_3$ cell performance with temperature and the thickness of the absorber layer.

The presence of an acceptor impurity in the $CSSnCl_3$ absorber layer, along with any lack of stoichiometry or flaws in the synthetic material, determines the concentration of the carrier.

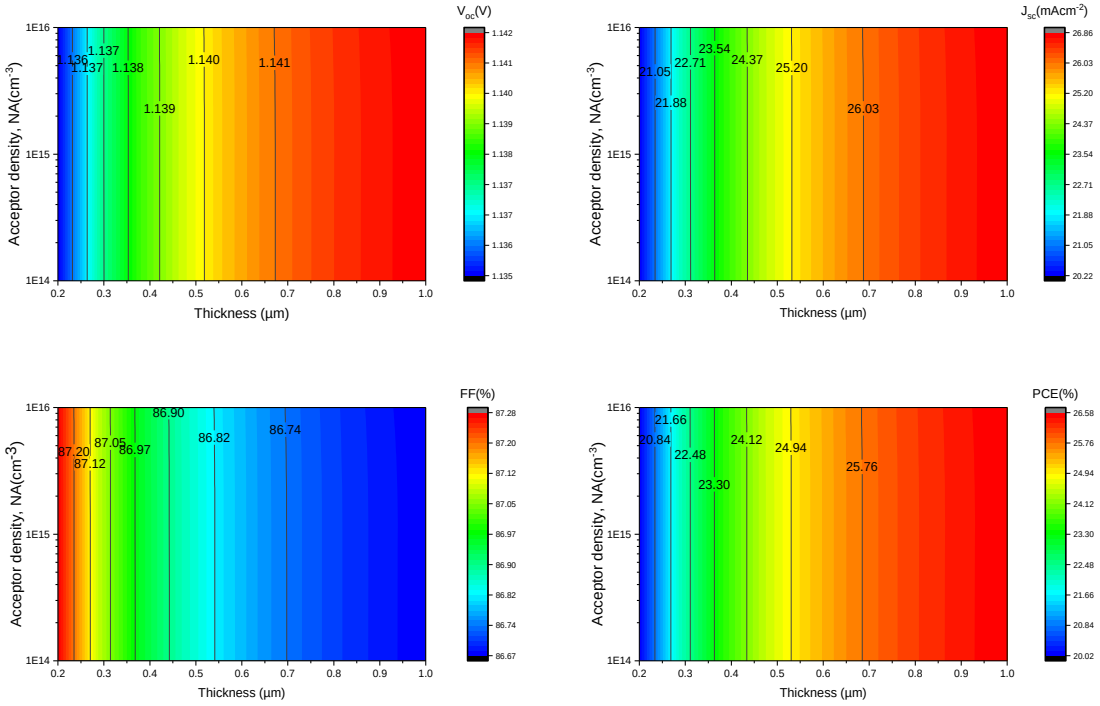

Figure 7. The effect of the thickness and acceptor density of $CSSnCl_3$ on the solar cell electrical properties.

In Figure 7, the influence of the absorber layer's thickness and doping concentration on the electrical characteristics of solar cells is illustrated. It can be observed that augmenting the doping concentration does not affect the electrical parameters. However, increasing the absorber layer's thickness enhances the internal electric field of solar cell devices, which is advantageous for achieving better values of the solar cell's V_{oc}, J_{sc}, and PCE.

5. CONCLUSION

The performance of $CsSnCl_3$ perovskite-type devices was evaluated using SCAPS-1D simulations with an AM1.5G solar spectrum and an operating temperature of 300 K. In these simulations, the effects of resistance, temperature, doping concentrations in the absorber and buffer layers, and the thickness of the layers on the PV properties of the devices were investigated. Increasing the doping concentration of CdS as a buffer layer in a solar cell can lead to a decrease in the power conversion efficiency (PCE) and short-circuit current, increasing the absorber layer's thickness enhances the internal electric field of solar cell devices, which is advantageous for achieving better values of the solar cell's V_{oc}, J_{sc}, and PCE. Al: ZnO/ ZnO/ CdS/ $CsSnCl_3$/ and MoS_2 hetero structure make up our design, which outperforms the others with a very good reported Power conversion of 26.15%.

References

1. Hossain, M.K., et al., An extensive study on multiple ETL and HTL layers to design and simulation of high-performance lead-free CsSnCl3-based perovskite solar cells. Scientific Reports, **13**(1): p. 2521(2023).

2. Rahmani, E.F., H. Aliah, and P. Pitriana. Phonon properties calculation of inorganic perovskite CsSnX3 (X= Cl, Br, I) in cubic phase using density functional theory (DFT). in AIP Conference Proceedings. AIP Publishing (2023).

3. Kumar, A., et al., Tenability and improvement of the structural, electronic, and optical properties of lead-free CsSnCl 3 perovskite by incorporating reduced graphene oxide (rGO) for optoelectronic applications. Journal of Materials Chemistry C, **11**(10): p. 3606-3615 (2023).

4. Mahassen, H.E. and M.M. SHABAT, STUDY OF SOLAR CELLS STRUCTURES BASED ON PEROVSKITE AND NANOPARTICLES. Proceedings of the Romanian Academy, Series A: Mathematics, Physics, Technical Sciences, Information Science **24** (1):(2023).

5. Elblbeisi, M.H. and M.M. Shabat, Comparison between different solar cells based on perovskite types. Israa University Journal of Applied Science, **6**(2) (2023).

6. McMeekin, D.P., et al., Intermediate-phase engineering via dimethylammonium cation additive for stable perovskite solar cells. Nature Materials, **22**(1): p. 73-83(2023.).

7. Yu, W., et al., Enhancement of visible light photocatalytic activity of Ag2O/F-TiO2 composites. Journal of Molecular Catalysis A: Chemical, **407**: p. 25-31(2015).

8. Azhar, M.R., H. Aliah, and P. Pitriana. Calculation of the electronic structure CsBX3 (B= Pb and Sn, X= Cl, Br and I) using density functional theory (DFT) method as the active material of perovskite solar cells. in AIP Conference Proceedings. AIP Publishing (2023).

9. Chen, Y.-J., C. Hou, and Y. Yang, Surface energy and surface stability of cesium tin halide perovskites: a theoretical investigation. Physical Chemistry Chemical Physics, **25**(15): p. 10583-10590 (2023).

10. Dwivedi, D., Modeling of CZTSSe solar photovoltaic cell for window layer optimization. Optik, **222**: p. 165407 (2020).

11. Kumar, R.R. and S.K. Pandey, Performance evaluation and material parameter perspective of eco-friendly highly efficient CsSnGeI3 perovskite solar cell. Superlattices and Microstructures, **135**: p. 106273(2019).

12. Raghvendra, R., R. Kumar, and S. Pandey, Performance evaluation and material parameter perspective of eco-friendly highly efficient CsSnGeI3 perovskite solar cell. Superlattices Microstruct., **135**(106273) (2019).

13. Tobbeche, S., et al., Improvement of the CIGS solar cell performance: structure based on a ZnS buffer layer. Optical and Quantum Electronics, **51**: p. 1-13(2019).

14. Ahmed, S., et al., Numerical development of eco-friendly Cs2TiBr6 based perovskite solar cell with all-inorganic charge transport materials via SCAPS-1D. Optik, **225**: p. 165765 (2021).

15. Kapadnis, R., et al., Cadmium telluride/cadmium sulfide thin films solar cells: a review. ES Energy & Environment, **10**(2): p. 3-12(2020).

16. Ashok, A., et al., Comparative studies of CdS thin films by chemical bath deposition techniques as a buffer layer for solar cell applications. Journal of Materials Science: materials in Electronics, **31**: p. 7499-7518 (2020).

17. Çiriş, A., et al., The effect of ZnCl2 and CdCl2 treatment on ZnS/CdS junction partner on CdTe cell performance. Materials Science in Semiconductor Processing, **149**: p. 106860(2022).

18. Lee, J.-H., et al., Electrical and optical properties of boron doped CdS thin films prepared by chemical bath deposition. Thin Solid Films, **431**: p. 344-348(2003).

19. Kakhaki, Z.M., et al., Influence of Cd salt concentration on the photoconductivity of CdS thin films prepared by chemical bath technique. Materials Science in Semiconductor Processing, **148**: p. 106773(2022).

20. Munna, F., et al., Effect of zinc doping on the optoelectronic properties of cadmium sulphide (CdS) thin films deposited by chemical bath deposition by utilising an alternative sulphur precursor. Optik, **218**: p. 165197(2020).